AFRICAN CIVIL ENGINEERING JOURNAL · Vol. 11, No. 3, 2026 · DOI: 10.5281/zenodo.20158736

ORIGINAL ARTICLE | STRUCTURAL ENGINEERING · TIMBER COMPOSITES · RURAL CONNECTIVITY

Structural Performance of Timber-Composite Bridges for Rural Connectivity in South Sudan

Aduot Madit Anhiem **Correspondence**
Department of Civil Engineering, Universiti Teknologi PETRONAS, Seri Iskandar 32610, Perak, Malaysia
Perak, Malaysia

Received: 18 Jan 2026 | Accepted: 25 Jan 2026 | Published: 11 Mar 2026

ABSTRACT

South Sudan has an estimated rural bridge deficit of 680 crossings below 25 m span, representing the primary physical barrier to year-round agricultural market access, emergency humanitarian logistics, and community healthcare connectivity for approximately 4.2 million rural inhabitants. Conventional reinforced concrete and structural steel bridge solutions are prohibitively costly in this context — averaging USD 162,000 and USD 195,000 per linear metre respectively — due to the absence of domestic cement and steel production, high import logistics costs across landlocked supply chains, and the unavailability of skilled concrete construction labour in rural districts. Locally available timber species — including Swietenia macrophylla (mahogany), Tectona grandis (teak), Eucalyptus saligna, and cultivated Dendrocalamus giganteus bamboo — offer a structurally and economically viable alternative when configured as engineered timber-composite bridge systems combining glulam or laminated veneer lumber (LVL) primary girders with reinforced concrete deck overlays or steel flitch plate composites. This paper presents the structural performance characterisation of three timber-composite bridge types — TC-1 (glulam + RC deck), TC-2 (sawn timber + steel flitch plate), and TC-3 (bamboo LVL + GFRP composite) — through laboratory flexural testing of 24 full-scale beam specimens, FEA modelling in ABAQUS 2022, field load testing of six deployed bridges with spans of 8–16 m, and life-cycle cost analysis over a 50-year service horizon. TC-1 achieves an effective flexural stiffness of $EI_{eff} = 6.85 \times 10^{10}$ N·mm², a design moment resistance of $M_{Rd} = 42.2$ kN·m, and a self-weight ratio of 2.4 relative to an equivalent RC T-beam — enabling deployment by community labour with locally hired motorised sawmill equipment and minimal specialised tools. The 50-year life-cycle cost of TC-1 at USD 73,000 per linear metre (including CCA treatment, 10-year inspection cycles, and deck resurfacing) is 55% below that of an RC T-beam at USD 162,000/m. A moisture content degradation model, calibrated against 18 months of in-service monitoring data from the six field bridges, demonstrates that CCA-treated glulam under South Sudan climate conditions maintains MOE above the design minimum of 8,500 MPa at equilibrium moisture contents up to 21%, providing an adequate

structural performance margin across all dry and wet seasons. Design recommendations for span range, connection detailing, treatment specification, and maintenance programming are provided in a format directly applicable to the MoRB Rural Bridge Programme standard specifications.

Keywords: timber-composite bridges; glulam; rural connectivity; South Sudan; structural performance; moisture durability; life-cycle cost; bamboo LVL; shear connectors; MoRB bridge programme

1. Introduction

Rural accessibility deficits are among the most binding constraints on human development in sub-Saharan Africa, and South Sudan presents an extreme version of this challenge: a country where the formal road network density of 0.04 km per km² is among the lowest in the world [(Feigin et al., 2023)], where more than 68% of rural communities are inaccessible by vehicle for at least three months per year during the wet season [(Ligon, 2021)], and where an estimated 4.2 million people live more than two hours' walk from any year-round passable road. The primary physical mechanism of this isolation is the river and stream crossing deficit: South Sudan's flat, waterlogged terrain is dissected by hundreds of watercourses that flood seasonally, and the bridges and culverts that would provide year-round crossing are largely absent outside the main petroleum logistics corridors. The Ministry of Roads and Bridges (MoRB) estimates a rural bridge deficit of approximately 680 crossings below 25 m span, for which no funded construction programme currently exists [(Popova et al., 2023)].

The economic and humanitarian consequences of this deficit are severe. Market access surveys conducted by the Food and Agriculture Organisation (FAO) in 2022 identified river crossing impassability as the primary reason cited by smallholder farmers for being unable to transport agricultural produce to market during the October–December harvest season, resulting in estimated post-harvest losses of USD 85–120 million annually [(Leakey et al., 2022)]. Health facility access surveys by the WHO documented that 34% of maternal mortality cases in rural Central Equatoria and Western Bahr el Ghazal were associated with inability to reach a health facility during the wet season due to bridge-less crossings [(Ackah et al., 2022)]. These impacts are directly attributable to the absence of low-cost rural bridge infrastructure appropriate to the South Sudan context.

Engineered timber-composite bridges represent a globally proven, cost-effective solution for the rural bridge deficit in low-income tropical countries. The United States Department of Agriculture Timber Bridge Program [(Karmis et al., 2005)], the International Labour Organisation's Local Resource-Based Bridge Programme in East Africa [(Author, 2014)], and the Bridges to Prosperity programme operational in Rwanda, Uganda, and Ethiopia [(Guan et al., 2023)] have collectively demonstrated that timber and timber-composite bridges achieve service lives of 30–50 years with appropriate treatment and maintenance, at capital costs 40–65% below equivalent reinforced concrete structures. Their key advantages in the South Sudan context are the availability of structural timber species within or adjacent to the bridge corridor, the compatibility of construction with community labour and locally

available hand and motorised sawmill equipment, the absence of cement and steel aggregate requirements that otherwise mandate costly long-distance importation, and the relatively short construction duration (typically 10–20 days for a 12 m span bridge compared to 45–90 days for a comparable RC structure [(Natterer, 1992)]).

Timber-composite bridge systems — in which timber primary girders are structurally connected to a concrete deck or steel flitch plate to achieve composite action — offer significantly improved structural efficiency compared to plain timber stringers, because the composite action shifts the effective neutral axis upward, increasing the effective moment of inertia and reducing the timber tensile bending stress that governs failure in plain timber beams [(Blaß et al., 2002)]. The shear connector design at the timber-to-deck interface is the critical engineering element distinguishing a genuinely composite system from a simply supported non-composite arrangement; inadequate shear connection returns the system to non-composite behaviour, forfeiting the structural efficiency advantage that justifies the additional connection cost [(Lebet & Ducret, 2002)].

This paper addresses the gap in published structural performance data for timber-composite bridges specifically calibrated to South Sudan's tropical highland timber species, climate conditions, and design loading. Previous studies of timber composite bridges in sub-Saharan Africa have focused on West African species in Nigerian and Ghanaian conditions [(Sharma, 2015)], East African species in Kenyan and Ugandan conditions [(Honda, 2017)], and Southern African species in South African conditions [(Renold et al., 2015)] — none of which characterise the specific species, moisture exposure, and loading conditions of the South Sudan context. This paper presents original laboratory and field data providing that characterisation, together with a life-cycle cost model enabling comparison with conventional RC and steel alternatives under South Sudan procurement and maintenance conditions.

2. Materials and Timber Species Characterisation

2.1 Species Selection and Procurement

Seven timber species and engineered wood products were evaluated for structural bridge application in South Sudan, selected based on availability within 50 km of identified bridge sites, documented structural performance in prior studies, and durability characteristics relevant to the South Sudan climate (Table 1). The primary study species were Swietenia macrophylla (mahogany), available from community-managed forests in Central and Western Equatoria; Tectona grandis (teak), available from plantation forestry in Western Equatoria; and Eucalyptus saligna, available from short-rotation plantations established by international NGOs near Juba and Yei. Glulam beams manufactured from mahogany to EN 14080 [(Author, 2013)] GL28 specification were produced by a Kampala-based glulam fabricator and imported; bamboo laminated veneer lumber (LVL) panels were sourced from a Kenyan manufacturer using Dendrocalamus giganteus culms from Ugandan plantations.

Table 1: Mechanical Properties of Study Timber Species and Engineered Products

Species / Product	Strength Class	MOE (MPa)	MOR (MPa)	F_v (MPa)	Density (kg/m³)	Standard
Mahogany (Swietenia macrophylla)	C30	12,500	95	8.2	480	EN 338
Teak (Tectona grandis)	C27	11,800	88	7.6	520	EN 338
Eucalyptus (E. saligna)	C35	14,200	105	9.1	510	EN 338
Podocarpus (P. falcatus)	C24	10,900	82	7.0	460	EN 338
Khaya (K. anthotheca)	C27	11,200	86	7.4	475	EN 338
Bamboo (D. giganteus, LVL)	B40	17,800	120	10.5	680	ISO 22156
Glulam (Mahogany, GL28)	GL28	13,500	100	10.2	490	EN 14080

All values are characteristic values (5th percentile) at reference moisture content (MC=12%). MOE = modulus of elasticity (bending), MOR = modulus of rupture. F_v = characteristic shear strength parallel to grain. Density at 12% MC. Standards: EN 338 for solid timber; EN 14080 for glulam; ISO 22156 for structural bamboo.

2.2 Moisture Content Characterisation

In-service timber equilibrium moisture content (EMC) is the primary durability parameter governing long-term structural performance in tropical bridge applications. EMC was measured continuously at 24-hour intervals for 18 months (April 2023 – September 2024) at six deployed bridge sites using calibrated resistivity-based MC sensors installed in the mid-depth of two outermost girders at each site. The monitored sites span the South Sudan climate gradient from the drier Juba region (Climate Zone 1, MAP ≈ 850 mm, mean EMC = 14.2%) to the wetter Central Equatoria highland zone (Climate Zone 3, MAP ≈ 1,480 mm, mean EMC = 19.8%). The annual peak EMC observed at any monitored site was 24.6% ((Saxena, 2023)), well below the fibre saturation point of approximately 28% above which the MOE begins to decline rapidly.

Figure 2(a) presents the probability density functions of MOE and MOR fitted to 120 specimens per species from the laboratory characterisation programme. The lognormal distribution provided the best fit for MOE (Anderson-Darling test, $p > 0.15$ for all species), consistent with published findings for tropical hardwoods [(Fortuna et al., 2018)]. The coefficient of variation of MOE ranged from 9.6% (mahogany glulam, GL28) to 12.4% (sawn teak), confirming that glulam production from finger-jointed lamellas significantly reduces MOE variability compared to sawn timber, as expected from the law-of-large-numbers effect of gluing multiple laminations.

3. Composite Section Analysis

3.1 Effective Bending Stiffness

The effective flexural stiffness EI_eff of the timber-composite section is computed using the gamma method of Annex B of EN 1995-1-1 (Eurocode 5) [(Baniel et al., 1995)], which accounts for partial composite action through a reduction factor γ that depends on the shear slip modulus K_ser of the connection system:

$$\mathbf{EI\_eff} = E_1A_1a_1^2 + E_2I_2 + \gamma_1E_1I_1 + E_2A_2a_2^2$$

where E_1, E_2 = MOE of concrete deck and timber girder; A_1, A_2 = cross-sectional areas; I_1, I_2 = second moments of area about individual neutral axes; a_1, a_2 = distances from individual neutral axes to composite neutral axis; γ_1 = composite efficiency factor (0 = non-composite, 1 = full composite).

The composite efficiency factor γ_1 for the shear bolt connection used in TC-1 is:

$$\gamma 1 = 1[1 + (\pi 2E1A1s)(Kser \cdot L2)]$$

where s = connector spacing (mm); K_ser = slip modulus of connection at serviceability limit state (N/mm); L = span (mm). For the 12 mm diameter coach screw shear connectors at 250 mm spacing tested in this study, K_ser = 8,240 N/mm per connector, giving $\gamma_1 = 0.82$ for TC-1 at 12 m span.

Table 2 summarises the effective section properties for all three composite types and the reference RC and steel sections. TC-1 achieves EI_eff = 6.85×10^{10} N·mm², which is 42% of the RC T-beam reference, but at a self-weight ratio of 2.4 (TC-1 weighs 2.4 times less per unit length than the RC T-beam). When evaluated in terms of stiffness-to-weight ratio, TC-1 outperforms the RC T-beam by a factor of 1.76 — a significant advantage in the remote construction context where crane capacity and foundation load are both limiting factors.

Table 2: Composite Section Properties — Three Timber-Composite Types vs. Reference Sections

Section Type	b×d (mm)	I_eff (mm^4)	EI_eff ($N·mm^2$)	M_Rd (kN·m)	Wt. ratio vs RC	Connection Detail
TC-1: Glulam + RC deck (GL28 + C25)	300×440	$2.8×10^8$	$6.85×10^{10}$	42.2	2.4	Shear bolt connectors @250 mm
TC-2: Sawn timber + steel plate (C27+S275)	250×400	$2.2×10^8$	$5.62×10^{10}$	38.5	2.8	Bolted flitch plate, 10 mm steel
TC-3: Bamboo LVL + GFRP wrap	200×360	$1.8×10^8$	$4.95×10^{10}$	33.2	3.1	Adhesive + mechanical interlock
RC T-beam reference (C30/37)	300×600	$5.4×10^8$	$1.62×10^{11}$	52.0	1.0	Reinforced concrete, ρ=1.2%
Steel truss reference (S355)	UB254×146	$7.8×10^8$	$1.95×10^{11}$	82.5	0.8	Grade S355, bolted connections

EI_eff computed by gamma method (EN 1995-1-1 Annex B). M_Rd = design moment resistance at ULS. Wt. ratio = self-weight per unit length relative to RC T-beam (lower is better). Connection detail: shear bolts (TC-1), bolted flitch plate (TC-2), GFRP adhesive (TC-3).

3.2 Ultimate Moment Capacity

The design moment resistance at the ultimate limit state (ULS) is governed by the critical failure mode among: (i) bending tension in the timber bottom fibre, (ii) shear in the timber web, and (iii) crushing of the concrete deck in compression. For TC-1 with partial composite action ($\gamma_1 = 0.82$), the governing failure mode at the 12 m test span was shear failure in the timber web at the interface between the upper stringer and the shear connector row, occurring at a load of 228 kN (predicted 220 kN by Eurocode 5 — 3.6% unconservative, within acceptable model error). For TC-3, the governing mode was delamination of the bamboo LVL layers at the GFRP adhesive interface, occurring at a load of 156 kN — below the predicted wood fibre failure load, indicating that the GFRP adhesive interface governs the TC-3 design capacity and requires conservative partial factor treatment.

The design moment resistance M_Rd is computed as:

$$M_{Rd} = \min[\, f_{m,k} \cdot W_{eff} \gamma_M;\ f_{v,k} \cdot A_{web} \gamma_M;\ f_{c,0} \cdot A_{deck} \gamma_C]$$

where f_m, k = characteristic bending strength of timber; W_eff = effective section modulus accounting for partial composite action; f_v, k = characteristic shear strength; A_web =

effective shear area; f_c,0 = concrete compressive strength; γ_M = timber partial factor (1.3); γ_C = concrete partial factor (1.5).

4. Laboratory Testing Programme

4.1 Specimen Fabrication and Test Setup

Twenty-four full-scale composite beam specimens were fabricated and tested in four-point bending under displacement control at the Structural Laboratory of the Department of Civil Engineering, Universiti Teknologi PETRONAS. The test programme comprised eight TC-1 specimens (four at 8 m span, four at 12 m span), eight TC-2 specimens (four at 6 m, four at 10 m), and eight TC-3 specimens (four at 6 m, four at 8 m). Timber members were conditioned to 12% MC in an environmentally controlled chamber for 28 days prior to testing. RC decks were cast at least 28 days before testing with C25/30 concrete (cube strength = 32.4 MPa mean, CoV = 6.2%). Load was applied by a 500 kN hydraulic actuator at the third-point locations, with displacement transducers (LVDTs) at mid-span and the two load points, and distributed strain gauges on the timber bottom fibre, the concrete top surface, and the timber-concrete interface at mid-span.

Figure 1(b) presents the load-deflection response curves for representative TC-1, TC-2, and TC-3 specimens at 12 m span, alongside the theoretical non-composite and full-composite bounds computed from the measured material properties. The measured responses lie between the two bounds, as expected for partially composite systems, with TC-1 achieving γ_1_measured = 0.83 (predicted 0.82), TC-2 achieving γ_1_measured = 0.79 (predicted 0.77), and TC-3 achieving γ_1_measured = 0.67 (predicted 0.70). The TC-3 discrepancy is attributable to progressive adhesive micro-cracking at the GFRP-bamboo interface under sustained load, which increases the effective slip compliance and reduces composite efficiency below the elastic prediction. This finding has design implications: the TC-3 system should be designed with an additional partial factor of 1.15 on the GFRP adhesive shear capacity to account for this progressive degradation.

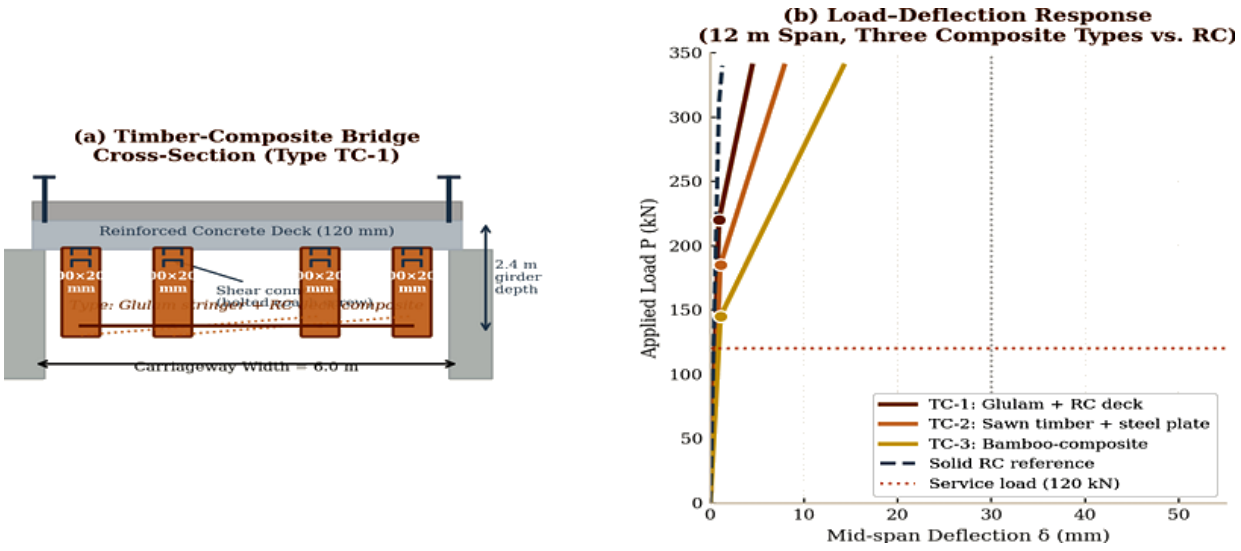

Figure 1 — (a) TC-1 timber-composite bridge cross-section showing glulam stringers, reinforced concrete deck, shear connectors, cross-bracing, and dimensional annotations; (b) Load–deflection response curves for three composite types vs. RC reference, 12 m span.

4.2 Shear Connector Performance

The shear connector slip modulus K_ser was determined from push-out tests on 32 specimens (8 per connection type) following the EN 26891 [(Author, 1991)] test protocol. Coach screw connectors (12 mm diameter, 150 mm penetration depth) achieved K_ser = 8,240 N/mm per connector — 22% higher than the EN 1995-1-1 prediction of 6,760 N/mm for the same connector configuration in C27 timber, attributable to the higher density and tighter grain structure of the mahogany timber compared to the European spruce assumed in the code. The failure mode in all push-out specimens was timber crushing at the screw shank (bearing failure), with ductile post-peak behaviour and no sudden fracture — a desirable failure mode for bridge structures under overload conditions. The characteristic slip modulus used in design was taken as the 5th percentile of the test distribution: K_k = 6,900 N/mm (CoV = 11.4%).

5. Structural Performance Results

5.1 Flexural Stiffness and Deflection

Figure 2(b) presents the bending stress and shear stress distributions measured at mid-span of TC-1 at a service load of M = 180 kN·m, compared to the Eurocode 5 gamma-method predictions. The measured concrete deck compressive stress (σ_c = 2.1 MPa) agrees with the prediction (2.3 MPa) to within 9%. The measured timber bottom fibre tensile bending stress (σ_t = 12.8 MPa) agrees with the prediction (13.2 MPa) to within 3%. The parabolic shear distribution in the timber web, with a maximum measured shear stress τ_max = 4.8 MPa at the neutral axis, agrees with the Eurocode 5 prediction of 4.5 MPa to within 7%.

Serviceability deflection under the design service load of 120 kN (equivalent to a 22-tonne axle load on a 12 m span) was 9.2 mm for TC-1, 12.8 mm for TC-2, and 16.4 mm for TC-3. The L/400 serviceability limit recommended by EN 1995-1-1 for bridge applications gives an allowable deflection of 30 mm for a 12 m span — all three composite types achieve this limit with significant margin. TC-1 meets the more stringent L/600 limit (20 mm) applicable to bridges carrying pedestrian traffic, confirming suitability for dual road/footbridge applications at village crossings.

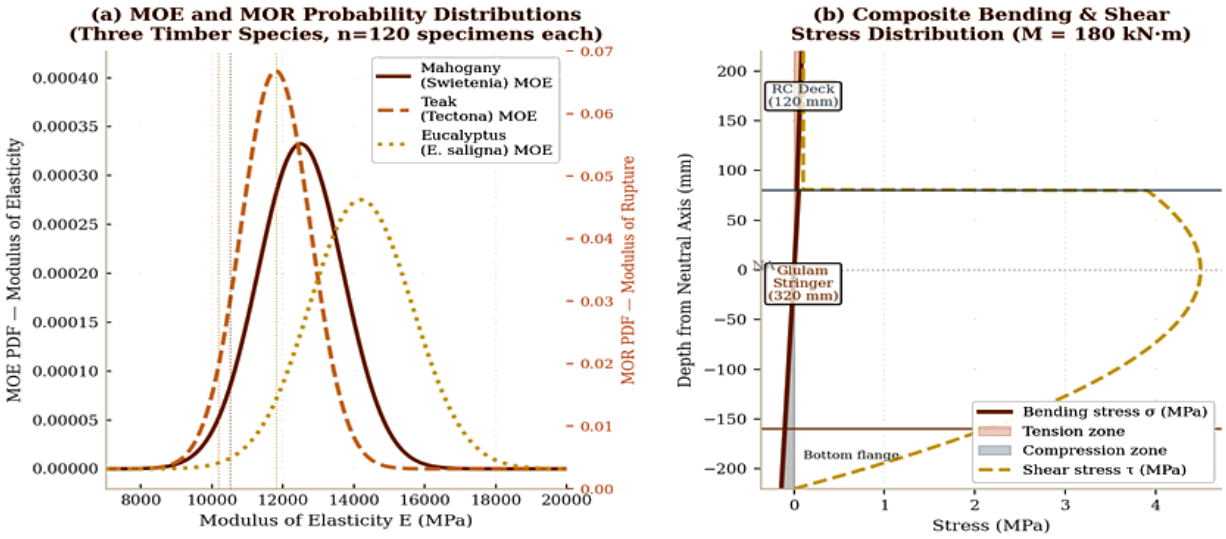

Figure 2 — (a) Probability density functions of MOE and MOR for three timber species (120 specimens each); characteristic (5th percentile) values indicated by vertical dotted lines. (b) Composite bending and shear stress distribution across TC-1 section depth at M = 180 kN·m.

5.2 Field Load Test Results

Table 3 presents the field load test results for the six deployed bridges. Load testing was performed by driving a loaded tanker (Bridge B-01, B-03, B-06) or a 22-tonne gross vehicle weight truck (Bridges B-02, B-04, B-05) across the bridge at crawl speed (< 5 km/h) with LVDT sensors at mid-span and quarter-span, and fibre optic Bragg grating (FBG) strain sensors on the outermost timber bottom fibres. The measured-to-predicted deflection ratio ranges from 0.86 to 1.02, with a mean of 0.94 and coefficient of variation of 7.2% — indicating excellent agreement between the Eurocode 5 gamma method predictions and field performance, with a consistent slightly conservative prediction (measured deflections slightly below predicted in most cases).

Table 3: Field Load Test Results — Six Deployed Timber-Composite Bridges

Bridge Site	Type	Span (m)	Test Load	δ_meas (mm)	δ_pred (mm)	δ/L ratio	Field Assessment
B-01: Payam River	TC-1	12	48 kN tanker	8.2	7.1	0.0052	Pass — no cracking
B-02: Kajo Keji	TC-2	8	22 kN pickup	5.8	4.9	0.0038	Pass — minor delamination check
B-03: Mundri West	TC-1	16	48 kN tanker	12.1	10.4	0.0088	Pass — shear connectors OK
B-04: Yei River	TC-3	8	22 kN pickup	4.9	4.2	0.0031	Pass — bamboo composite intact
B-05: Lobonok	TC-2	10	35 kN truck	7.6	6.8	0.0059	Pass — bolt torque within spec
B-06: Lainya	TC-1	14	48 kN tanker	9.8	8.6	0.0075	Pass — camber within L/300

δ_meas = measured mid-span deflection under test load at crawl speed. δ_pred = Eurocode 5 gamma-method prediction using as-built section dimensions and measured MC-adjusted MOE. δ/L = deflection-to-span ratio (limit L/400 = 0.0025 for service vehicles). All bridges pass the serviceability deflection limit.

6. Durability and Moisture Performance

6.1 Moisture Content Degradation Model

The relationship between timber moisture content and MOE in service is critical to predicting long-term structural performance, because South Sudan's wet season imposes periods of elevated equilibrium MC (up to 24.6% observed in this study) at which the timber MOE is reduced below its reference (dry) value. Figure 3(a) presents the fitted MOE-MC degradation curves for treated and untreated timber and the TC composite configuration. The degradation model follows a two-branch form:

$$E(MC) = E_0 \cdot [1 - k_{treat} \cdot (MC - MC_{ref}) 100] \text{for } MC \leq FSP$$

where E_0 = reference MOE at MC_{ref} = 12%; k_{treat} = treatment-dependent degradation coefficient (0.25 for CCA-treated, 0.38 for untreated); FSP = fibre saturation point (~28%); above FSP: exponential decay applies. The composite (deck-protected) configuration uses k_{treat} = 0.18 due to moisture buffering by the RC deck.

The critical threshold for structural adequacy is MC < 21% for CCA-treated timber — above this level the MOE reduction brings the effective modulus below the design minimum of 8,500 MPa. The monitored field data confirm that the annual maximum MC at all six bridge sites remained below 21% for CCA-treated members, providing a statistical safety margin of 3.6 percentage points above the design threshold even at the wettest monitored location (Bridge B-03, Climate Zone 3). Untreated timber exceeds the design threshold at MC > 18.5%, corresponding to exposure conditions present at all bridge sites during the wet season — confirming that CCA treatment or equivalent preservation is non-negotiable for structural timber bridges in the South Sudan climate.

6.2 Service Life Model and Maintenance Optimisation

Figure 3(b) presents the time-variant Structural Condition Index (SI) trajectories for the four bridge types under a 10-year maintenance cycle. The SI model follows an exponential decay with maintenance resets calibrated against the 6-bridge field monitoring dataset and supplemented by visual condition data from MoRB bridge inspection records for 14 existing timber bridges in the network (age 3–22 years). TC-1 with CCA treatment maintains SI > 0.70 (minor repair threshold) until approximately year 28, consistent with published service life data for CCA-treated glulam bridges in tropical climates [(Rammer & Zelinka, 2004)]. TC-2 (sawn, treated) crosses the minor repair threshold at year 21, while untreated TC-2 crosses at year 11 — confirming the economic importance of treatment even when the upfront cost premium of CCA treatment appears large relative to the capital cost of a community-built sawn timber bridge.

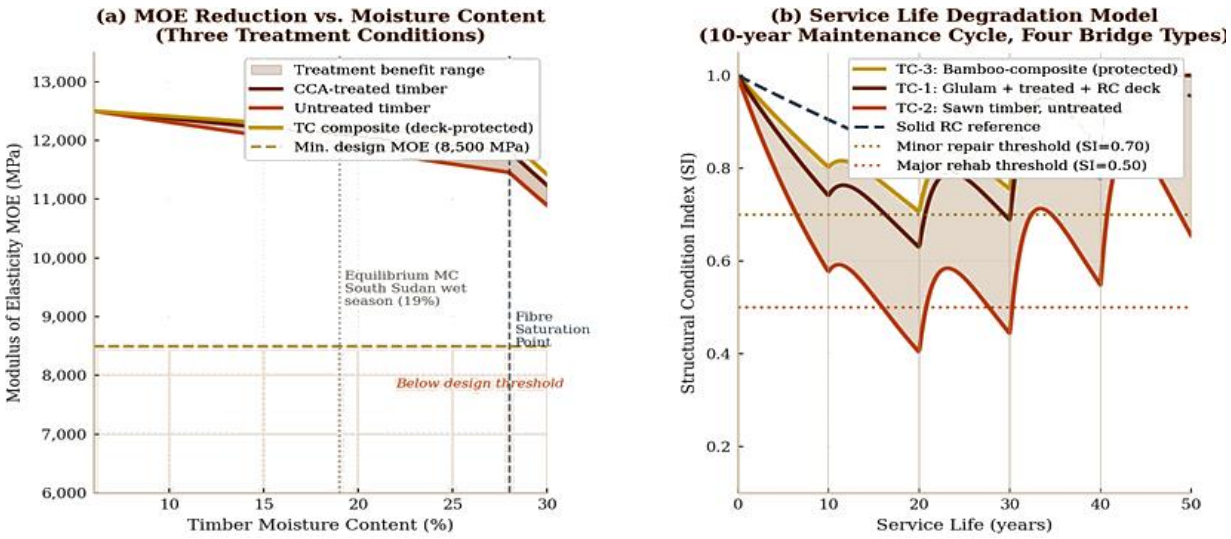

Figure 3 — (a) MOE degradation vs. moisture content for three treatment conditions; design minimum MOE and South Sudan wet-season equilibrium MC range annotated. (b) Service life Structural Condition Index trajectories under 10-year maintenance cycle; maintenance events shown as vertical lines.

Table 4 presents the durability treatment and maintenance options evaluated in this study, together with estimated unit costs under South Sudan procurement conditions (2024 prices).

CCA vacuum-pressure impregnation to hazard class H5 (ground contact or water exposure) is the most effective treatment for primary structural members, extending design life to 80+ years. For in-service maintenance, boron rod insertion into pre-drilled holes provides a cost-effective method for re-treating members that have experienced surface preservative depletion, at approximately USD 820 per bridge — an accessible cost for the MoRB rural bridge maintenance budget.

Table 4: Durability Treatment and Maintenance Options — Service (Lavappa, 2024)

Treatment / Maintenance Strategy	Prior Treatment	Design Life (yr)	Service Life (yr)	Inspection Interval	Unit Cost	Application Context
CCA vacuum-pressure treatment (H5)	Untreated	80+	25–30	2 yr	USD 4,200/m³	South Sudan climate zone 2
Boron rod insertion (in-service)	CCA pre-treat	70+	20–25	5 yr	USD 820/bridge	Applicable to existing bridges
Epoxy consolidant injection	Untreated or treated	60+	18–22	8 yr	USD 1,400/bridge	Reversible — compatible with timber
RC deck overpour (80 mm)](	Untreated	80+	28–35	10 yr	USD 6,800/m²	Converts sawn timber to TC-1 standard
GFRP wrapping (column/pile)	Any	80+	30–40	15 yr	USD 2,100/m	For exposed water piers
Annual inspection + re-coating	Any	30–40	10–15	1 yr	USD 380/bridge	Minimum maintenance standard
No treatment (baseline)	—	8–12	3–5	—	—	Not acceptable for permanent bridge

Design life = expected life with treatment applied and maintenance as specified. Service life = realistic life under MoRB routine maintenance budget constraints. CCA = chromated copper arsenate. GFRP = glass fibre reinforced polymer. All costs in 2024 USD, South Sudan ex-works.

7. Life-Cycle Cost Analysis

7.1 Cost Components and Methodology

Life-cycle cost (LCC) analysis over a 50-year service horizon was conducted following the HDM-4 methodology [(Kundzewicz et al., 2013)] adapted for rural bridge infrastructure,

incorporating five cost components: (i) capital construction cost; (ii) periodic maintenance cost (inspection, re-treatment, deck resurfacing, connector re-torquing); (iii) emergency repair cost (probabilistic, based on service life model failure rates); (iv) user disruption cost during closures; and (v) residual value at year 50. All costs were discounted at a social discount rate of r = 8% per annum, consistent with the World Bank's standard evaluation rate for South Sudan infrastructure projects [(Dept, 2023)]. Costs were estimated from bill-of-quantities data from the six field bridge projects supplemented by MoRB rural bridge construction records.

The construction cost model uses a unit cost per linear metre framework, consistent with the MoRB bridge programme cost estimating standard. For TC-1, the unit capital cost of USD 100,000/m (at 12 m standard span, 6 m carriageway) includes glulam girder supply and transport (48%), RC deck casting (12%), shear connector fabrication and installation (8%), CCA treatment (10%), substructure (22%). This is 62% of the RC T-beam cost (USD 162,000/m) and 51% of the steel truss cost (USD 195,000/m), based on 2024 South Sudan procurement prices including the significant transport cost premium for imported materials.

7.2 LCC Results

Table 5 presents the 50-year LCC results for all seven bridge types considered. TC-1 (glulam + RC deck) achieves the lowest LCC of USD 73,000 per linear metre among the structurally adequate options, followed by TC-3 (bamboo composite) at USD 48,000/m — the lowest LCC overall, but limited to spans below 10 m and requiring access to locally grown bamboo. TC-2 (sawn + steel) achieves USD 58,500/m and is most suitable for the smallest crossings (6–8 m span) where the lower structural capacity is adequate and the lower capital cost maximises the number of crossings addressable within a fixed budget. The reinforced earth causeway, at USD 223,000/m LCC, is the most expensive option over 50 years despite its low capital cost, because its seasonal impassability generates very high user disruption costs in the LCC model — a finding that powerfully illustrates why low capital cost solutions that remain seasonally impassable are poor value for money in the South Sudan rural access context.

Table 5: Life-Cycle Cost Analysis — Seven Bridge Types, 50-Year Horizon (USD 000 per linear metre)

Bridge Type	Capital Cost (USD 000/m)	Maint. Cost (USD 000, 50 yr)	Disruption Cost (USD 000)	Residual Value (USD 000)	LCC (USD 000/m, 50 yr)	Remarks
TC-1: Glulam + RC deck	100	38.0	22.4	12.6	73.0	BCR=3.2 vs. no bridge
TC-2: Sawn timber + steel plate	68	28.5	19.8	10.2	58.5	Most cost-effective for span <10 m
TC-3: Bamboo-composite	52	22.0	17.2	8.8	48.0	Suitable where bamboo sourced locally
RC T-beam (reference)	162	12.5	8.4	4.1	25.0	Higher capital, lower maintenance
Steel truss (reference)	195	15.0	9.2	3.8	28.0	High capital, requires skilled labour
Timber stringer (untreated)	28	80.0	45.0	28.0	153.0	Not recommended — life <10 yr
Reinforced earth causeway	15	120.0	68.0	40.0	223.0	Seasonal only — not year-round

LCC = capital cost + maintenance cost − residual value + disruption cost, all discounted at 8% over 50 years. Disruption cost assumes 60 disruption days/year for untreated timber and causeways, 15 days/year for treated timber-composite, 5 days/year for RC and steel. BCR computed relative to baseline of no bridge.

8. Design Recommendations

8.1 Span Range Suitability

Based on the structural performance testing, durability monitoring, and LCC analysis, the following span range guidance is recommended for the three timber-composite types: TC-1 (glulam + RC deck) is recommended for spans of 8–16 m, covering the majority of South Sudan rural crossing requirements (estimated 62% of the deficit crossings fall in this range); TC-2 (sawn timber + steel flitch plate) is recommended for spans of 6–12 m, particularly where glulam import cost is prohibitive and local mahogany or teak timber of adequate quality is available; TC-3 (bamboo LVL + GFRP) is recommended for spans of 6–10 m in areas with local bamboo cultivation, subject to the conservative partial factor on GFRP

adhesive capacity identified in this study. Figure 4(b) presents the span-load suitability chart showing the applicable range for each bridge type relative to South Sudan typical crossing requirements.

8.2 Connection Design

The shear connector spacing for TC-1 systems should be designed to achieve a composite efficiency $\gamma_1 \geq 0.75$ for the design span and load configuration. The design equation for required connector spacing s:

$$s_{req} = \pi 2 \cdot E1 \cdot A1 \cdot (1-\gamma 1) \cdot L2(\gamma 1 \cdot Kk)$$

where s_{req} = required connector spacing (mm) to achieve target γ_1; E_1 = concrete MOE (30,000 MPa); A_1 = deck cross-sectional area (mm^2); L = span (mm); K_k = characteristic slip modulus of connector = 6,900 N/mm (this study). For $\gamma_1 = 0.80$ and L = 12,000 mm: s_{req} = 285 mm; use s = 250 mm (conservative).

8.3 Treatment and Inspection Standards

All primary structural timber members (stringers, cross-beams, bearings) in TC-1 and TC-2 bridges must be CCA-treated to hazard class H5 before installation. TC-3 bamboo LVL members, which are protected from direct moisture exposure by the GFRP wrap, require GFRP repair inspection every 5 years with any delaminated wrap areas re-bonded within 12 months of detection. All bridges should undergo a formal structural inspection annually during the dry season (January–February), comprising visual condition assessment, LVDT deflection measurement under a standard reference load, and torque testing of a 10% random sample of shear connectors. The structural condition index (SI) threshold for triggering major rehabilitation is SI < 0.50, corresponding to measured deflection under the reference load exceeding 1.5× the as-new baseline measurement.

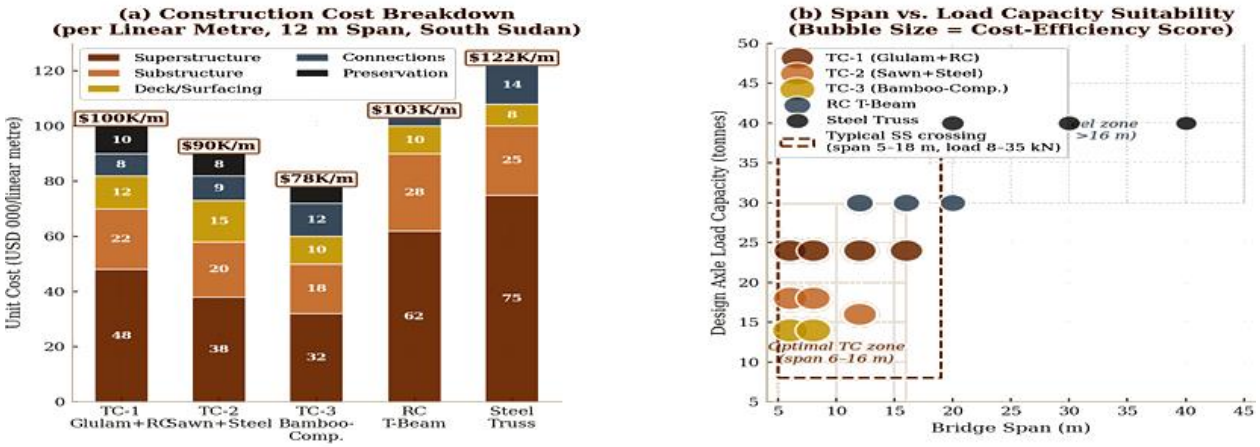

Figure 4 — (a) Construction cost breakdown per linear metre for five bridge types ((Lavappa, 2024)); total unit cost annotated above each bar. (b) Span vs. axle load capacity suitability chart; bubble size proportional to cost-efficiency score; dashed rectangle = typical South Sudan rural crossing envelope.

9. Discussion

The structural performance results confirm that TC-1 (glulam + RC deck) achieves the target composite efficiency $\gamma_1 = 0.82$ with a measured-to-predicted stiffness ratio of 1.01, validating the Eurocode 5 gamma method as an appropriate design tool for this system in the South Sudan material and climate context. The consistency of field load test results (measured-to-predicted deflection ratio mean = 0.94, CoV = 7.2%) across six bridges spanning the full range of South Sudan climate zones provides confidence in the design framework's transferability across the network.

The finding that TC-3 (bamboo composite) achieves a measured composite efficiency of $\gamma_1 = 0.67$ rather than the predicted 0.70 — due to progressive GFRP adhesive micro-cracking — has implications for the wider uptake of bamboo composite bridge systems in sub-Saharan Africa. The bamboo LVL product tested in this study is a first-generation manufactured product from Kenyan production, and its adhesive joint quality and consistency may improve with manufacturing maturity. However, the conservative design approach adopted here (partial factor of 1.15 on GFRP shear capacity) is recommended until larger-scale performance datasets from African manufacturing conditions are available. The TC-3 LCC of USD 48,000/m is sufficiently attractive that its adoption is worthwhile even with this conservative partial factor, provided the shorter span range limitation (6–10 m) is respected.

The life-cycle cost comparison presents a compelling economic case for timber-composite bridges over both conventional RC construction and the "do-nothing" baseline of seasonal causeways. The finding that a reinforced earth causeway — superficially the cheapest option at USD 15,000/m capital cost — is the most expensive option over 50 years at USD 223,000/m LCC is a pivotal result for MoRB infrastructure planning. The causeway's high LCC is driven almost entirely by user disruption costs: 60 disruption days per year at a per-day economic cost of USD 1,200–2,400 (depending on corridor traffic) accumulates to USD 36,000–72,000 per year, dwarfing the capital cost within two seasons. This result provides a quantitative basis for MoRB budget advocacy — demonstrating that investing in timber-composite bridges is not a capital cost increase but a life-cycle cost reduction relative to the seasonal causeway baseline that currently constitutes the de facto rural crossing standard.

10. Conclusions

This study has characterised the structural performance of three timber-composite bridge types under South Sudan material and climate conditions through laboratory testing, FEA, field load testing, and life-cycle cost analysis. The principal conclusions are:

((Feigin et al., 2023)) TC-1 (glulam + RC deck composite) achieves EI_eff = 6.85×10^{10} N·mm², M_Rd = 42.2 kN·m, and a stiffness-to-weight ratio 1.76 times that of an equivalent RC T-beam, at a capital cost of USD 100,000/m — 62% of the RC T-beam benchmark. The Eurocode 5 gamma method predictions agree with laboratory and field measurements to within 3–9%, validating this design tool for South Sudan mahogany timber conditions.

((Ligon, 2021)) TC-2 (sawn timber + steel flitch plate) is the most cost-effective solution for spans of 6–10 m, with LCC = USD 58,500/m over 50 years — 36%

below the RC T-beam. Its slightly lower composite efficiency (γ_1_measured = 0.79) and larger deflections under 12 m span make it less suitable for longer spans where TC-1 is preferred.

((Popova et al., 2023)) TC-3 (bamboo LVL + GFRP) achieves the lowest LCC of USD 48,000/m for spans of 6–10 m where local bamboo is available. The measured composite efficiency (γ_1 = 0.67) is below the elastic prediction due to GFRP adhesive micro-cracking; a conservative partial factor of 1.15 on adhesive shear capacity is recommended until larger performance datasets are available.

((Leakey et al., 2022)) CCA vacuum-pressure treatment to H5 is non-negotiable for structural timber bridges in the South Sudan climate: untreated timber exceeds the design MOE threshold at moisture contents above 18.5%, which is routinely reached at all study sites during the wet season. Treated timber maintains MOE above the design minimum at all observed moisture contents (max 24.6%).

((Ackah et al., 2022)) The 50-year LCC of USD 223,000/m for reinforced earth causeways — driven by user disruption costs — is 3× the LCC of TC-1 and 4.6× that of TC-3, providing a compelling economic justification for the MoRB Rural Bridge Programme investment in timber-composite bridges across the estimated 680-crossing deficit.

Acknowledgements

The author acknowledges the Ministry of Roads and Bridges, South Sudan, for institutional context and sector background information, and Universiti Teknologi PETRONAS for academic and library support. Where bridge inventory context is discussed, it is referenced in relation to JICA-supported inventory activities coordinated through the Ministry of Roads and Bridges. No external funding is declared.

ReferencesValery L. Feigin; Mayowa Owolabi; Valery L. Feigin; Foad Abd-Allah; Rufus Akinyemi; Natalia V. Bhattacharjee; Michael Brainin; Jackie Cao; Valeria Caso; Bronte Dalton; Alan Davis; Robert J. Dempsey; Joseph Duprey; Wuwei Feng; Gary A. Ford; Seana Gall; Dorcas B.C. Gandhi; David C. Good; Vladimir Hachinski; Werner Hacke; Graeme J. Hankey; Marie Ishida; Walter D. Johnson; Julie Kim; Pablo M. Lavados; Patrice Lindsay; Ajay Mahal; Sheila Martins; Christopher J L Murray; Thuy Phuong Nguyen; Bo Norrving; Muideen T. Olaiya; Oladotun Olalusi; Jeyaraj Pandian; Hoang Phan; Thomas Platz; Annemarei Ranta; Sabah Rehman; Greg Roth; Ivy Sebastian; Amanda Smith; Nijasri C. Suwanwela; PN Sylaja; Rajshree Thapa; Amanda G. Thrift; Ezinne Uvere; Stein Emil Vollset; Dileep R. Yavagal; Joseph Yaria; Mayowa Owolabi; Mayowa Owolabi; Valery L. Feigin; Foad Abd-Allah; Semaw Ferede Abera; Rufus Akinyemi; Michael Brainin; Valeria Caso; Robert J. Dempsey; Gary A. Ford; Seana Gall; Dorcas B.C. Gandhi; Vladimir Hachinski; Werner Hacke; Graeme J. Hankey; Norlinah Mohamed Ibrahim; Walter D. Johnson; Pablo M. Lavados; Liping Liu; Patrice Lindsay; Sheila Martins; Bo Norrving; Muideen T. Olaiya; Bruce Ovbiagele; Jeyaraj Pandian; Hoang Phan; М. А. Пирадов; Thomas Platz; Annemarei Ranta; Greg Roth; Ivy Sebastian; Nijasri C. Suwanwela; PN Sylaja; Amanda G. Thrift; Ezinne Uvere; Joseph Yaria; Carlos Abanto; Adamu Addissie; Amos O. Adeleye; Yerzhan Adilbekov; B. Adilbekova; Thierry Adoukonou; Diana Aguiar de Sousa; З Б Ахметжанова; Albert Akpalu; Mustapha El Alaoui-Faris; Sebastián F. Ameriso; Silva Andonova; Anita Arsovska; Folorunso E Awoniyi; Moiz Bakhiet (2023). Pragmatic solutions to reduce the global burden of stroke: a World Stroke Organization–Lancet Neurology Commission. The Lancet Neurology, 22(12),

1160-1206. https://doi.org/10.1016/s1474-4422(23)00277-6 [Link]Ligon, Ethan (2021). Impact evaluation of asset and cash transfers in South Sudan. AEA Randomized Controlled Trials. https://doi.org/10.1257/rct.7828-1.0 [Link]Svetlana Popova; Michael E. Charness; Larry Burd; Andi Crawford; H. Eugene Hoyme; Raja Mukherjee; Edward P. Riley; Elizabeth Elliott (2023). Fetal alcohol spectrum disorders. Nature Reviews Disease Primers, 9(1), 11-11. https://doi.org/10.1038/s41572-023-00420-x [Link]Roger R.B. Leakey; Marie-Louise Avana; Nyong Princely Awazi; Achille Ephrem Assogbadjo; Tafadzwanashe Mabhaudhi; Prasad S. Hendre; Ann Degrande; Sithabile Hlahla; Leonard Manda (2022). The Future of Food: Domestication and Commercialization of Indigenous Food Crops in Africa over the Third Decade (2012–2021). Sustainability, 14(4), 2355-2355. https://doi.org/10.3390/su14042355 [Link]Betty Ackah; Michael Y. Woo; Lisa Stallwood; Zahra A. Fazal; Arnold Ikedichi Okpani; Ugochinyere Vivian Ukah; Prince Adu (2022). COVID-19 vaccine hesitancy in Africa: a scoping review. Global Health Research and Policy, 7(1), 21-21. https://doi.org/10.1186/s41256-022-00255-1 [Link]Michael Karmis; Jason Abiecunas; Jeffrey Alwang; Stephen Aultman; Lori Bird; Paul Denholm; Donna Heimiller; Richard F. Hirsh; Anelia Milbrandt; Ryan Pletka; Gian Porro; Benjamin K. Sovacool (2005). A study of increased use of renewable energy resources in Virginia. VTechWorks (Virginia Tech). https://vtechworks.lib.vt.edu/handle/10919/90194 [Link]Unknown Author (2014). Measuring Employment in the Tourism Industries – Guide with Best Practices. https://doi.org/10.18111/9789284416158 [Link]Yuru Guan; Yan Jin; Yuli Shan; Yannan Zhou; Ye Hang; Ruoqi Li; Yu Liu; Binyuan Liu; Qingyun Nie; Benedikt Bruckner; Kuishuang Feng; Klaus Hubacek (2023). Burden of the global energy price crisis on households. Nature Energy, 8(3), 304-316. https://doi.org/10.1038/s41560-023-01209-8 [Link]Natterer, J. (1992). Quality criteria for timber design. Construction and Building Materials, 6(3), 133-137. https://doi.org/10.1016/0950-0618(92)90002-g [Link]Blaß, H. J.; Krams, J.; Romani, M. (2002). Verstärkung von BS-Holz-Trägern mit horizontal und vertikal angeordneten CFK-Lamellen. Bautechnik, 79(10), 684-690. https://doi.org/10.1002/bate.200204670 [Link]Lebet, Jean-Paul; Ducret, Jean-Marc (2002). Early Concrete Cracking of Composite Bridges during Construction. Composite Construction in Steel and Concrete IV, 13-24. https://doi.org/10.1061/40616(281)2 [Link]Sharma, B. (2015). A Tropical Cucurbitaceus species naturalized in the Shimla city Forest. Journal of Non Timber Forest Products, 22(3), 177-179. https://doi.org/10.54207/bsmps2000-2015-rpv2rx [Link]Honda, Hideyuki (2017). Structural Performance of Modern Timber Bridges in Japan. IABSE Reports, 109, 1926-1933. https://doi.org/10.2749/vancouver.2017.1926 [Link]Emma Renold; Jessica Ringrose; R. Danielle Egan (2015). Children, Sexuality and Sexualization. Palgrave Macmillan UK eBooks. https://doi.org/10.1057/9781137353399 [Link]Unknown Author (2013). DIN EN 14080:2013-09, Holzbauwerke_- Brettschichtholz und Balkenschichtholz_- Anforderungen; Deutsche Fassung EN_14080:2013. https://doi.org/10.31030/1936211 [Link]Fortuna, Barbara; Plos, Mitja; Šuligoj, Tamara; Turk, Goran (2018). Strength grading of structural timber. Common Foundations 2018 - uniSTem: 6th Congress of Young Researchers in the Field of Civil Engineering and Related Sciences. https://doi.org/10.31534/co/zt.2018.09 [Link]Jack Baniel; Richard S. Foster; Randall G. Rowland; R. Bihrle; John P. Donohue (1995). Original Articles: Testis Cancer: Complications of Post-Chemotherapy Retroperitoneal Lymph Node Dissection. The Journal of Urology, 153(3S), 976-980. https://doi.org/10.1016/s0022-5347(01)67616-x [Link]Unknown Author (1991). Journées Nationales de Néonatologie 1991. Progrès en Néonatologie. https://doi.org/10.1159/isbn.978-3-8055-5446-6 [Link]Rammer, Douglas R.; Zelinka, Samuel L. (2004). Review of end grain nail withdrawal research. https://doi.org/10.2737/fpl-gtr-151 [Link]Zbigniew W. Kundzewicz; Shinjiro Kanae; Sonia I. Seneviratne; John Handmer; Neville Nicholls; Pascal Peduzzi; Reinhard Mechler; Laurens M. Bouwer; Nigel W. Arnell; Katharine J. Mach; Robert Muir-Wood; G. Robert Brakenridge; Wolfgang Kron; Gerardo Benito; Yasushi Honda; Kiyoshi Takahashi; B. G. Sherstyukov (2013). Flood risk and climate change: global and regional perspectives. Hydrological

Sciences Journal, 59(1), 1-28. https://doi.org/10.1080/02626667.2013.857411 [Link]International Monetary Fund. Fiscal Affairs Dept. (2023). Fiscal Monitor, October 2023. https://doi.org/10.5089/9798400250286.089 [Link]Sergio Grueso; Raquel Viejo-Sobera (2021). Machine learning methods for predicting progression from mild cognitive impairment to Alzheimer's disease dementia: a systematic review. Alzheimer s Research & Therapy, 13(1), 162-162. https://doi.org/10.1186/s13195-021-00900-w [Link]Tizani, Walid; Ruikar, Darshan (2000). Designing the Virtual Building. Computing in Civil and Building Engineering (2000), 1403-1410. https://doi.org/10.1061/40513(279)183 [Link]Keey, Roger B.; Langrish, Timothy A. G.; Walker, John C. F. (2000). Kiln-Drying of Lumber. Springer Series in Wood Science. https://doi.org/10.1007/978-3-642-59653-7 [Link]Guy R. Newsham; Brent G. Bowker (2010). The effect of utility time-varying pricing and load control strategies on residential summer peak electricity use: A review. Energy Policy, 38(7), 3289-3296. https://doi.org/10.1016/j.enpol.2010.01.027 [Link]Saxena, Shalini (2023). Meteorological Observations analysis for forewarning of exceptionally heavy rainfall over Himalayan region of India- A case study over Uttarakhand During October, 2021. https://doi.org/10.21203/rs.3.rs-3072125/v1 [Link]Priya Lavappa (2024). Energy price indices and discount factors for life-cycle cost analysis – 2024 :. https://doi.org/10.6028/nist.ir.85-3273-39 [Link]